Acta Cryst. (1971). A27, 140

The Influence of Temperature on the MgO Zone-Axis Pattern

BY P. GOODMAN

Division of Chemical Physics, CSIRO, Chemical Research Laboratories, P.O. Box 160, *Clayton, Victoria* 3168, *Australis*

(*Received* 7 *October* 1968 *and in revised form* 16 *June* 1970)

Measurements made on convergent-beam patterns from MgO taken near the [001] zone-axis at two fixed temperatures have been studied in detail. Two types of patterns, namely the symmetrical excitation of a single 200 reflexion and the simultaneous excitation of the 200, 020, 220, reflexions were studied, using up to 129 beams in the dynamical calculations.

The absorption function, $V_h^i \exp(-B^i S^2)$, was found to be well defined at the zone axis, allowing separate determination of V_h^i and B^i. For the pattern for single excitation, $V_0^i = 0{\cdot}6$ volt, $V_h^i = 0{\cdot}14$ volt, $B^i = B = 0{\cdot}3$, was determined at room temperature. In comparing the two types of pattern at high temperature an increase in V_h^i of between two and three times was found for the 3-reflexion pattern. This increase, and the more normal value found for the single excitation pattern, seems to accord with other experience that the dynamical increase in V_h^i, as predicted by Yoshioka and Kainuma, possibly occurs in the vicinity of a many-line intersection of the Kossel pattern but not at the zone axis.

Introduction

In an earlier study of MgO from convergent-beam patterns data obtained at one temperature were analysed with the $\{h00\}$ systematic calculation (Goodman & Lehmpfuhl, 1967). More recent work has shown that, at least for MgO, this calculation gives the correct extinction length for certain orientations, but is much less helpful in interpreting the absorption measurements (Goodman & Johnson, 1970; Goodman, 1970). The zone-axis patterns would appear to have a great advantage due to their high symmetry. Present investigations with MgO indicate no particular advantage for the determination of individual structure factors; these may be found to within 1% from the simpler one-dimensional patterns so long as conclusions are supported finally by adequate 2- or 3-dimensional dynamical calculations for the particular projection. However they allow a much better analysis of the thermal parameters, *viz.* the Debye–Waller factor and the phenomenological absorption function, V_h^i, free from significant but relatively uninformative weak beam effects present in general orientations. The larger dynamical calculations are of course necessary at the outset, but use of symmetry lines reduces the complexity of both calculation and measurement.

For the present study patterns were taken at two well-defined temperatures at various points on the Kossel map with the 200 reflexion excited, to find phenomenological values for the Debye–Waller factor B, and V_h^i. The latter results have been tabulated separately (Goodman & Johnson, 1970). At first a B factor for room temperature found from X-ray diffraction, and structure factors for the [001] projection published by Togawa (1964) which also agreed with the previous analysis (Goodman & Lehmpfuhl, 1967) were assumed. Later the B factor was confirmed from the analysis; also the previous method of analysis has been improved by calculations allowing corrections for accidental interactions, and by more accurate wavelength determination from the Kossel map

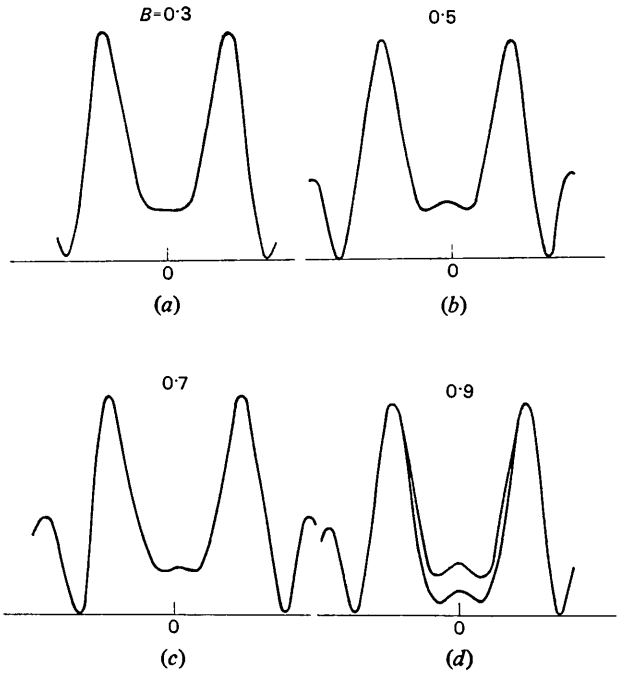

Fig. 1. Influence of B (Debye–Waller factor) value as shown by calculated 200 rocking curves from 4-beam systematic-interaction computation (analogue computer) for 105 kV and $D = 930$ Å. $B = 0{\cdot}3$, $0{\cdot}5$, $0{\cdot}7$, $0{\cdot}9$, for (*a*) to (*d*) respectively. In (*a*) to (*c*) $V_h^i = 0{\cdot}34$ volt. (*d*) shows calculations for $V_h^i = 0{\cdot}34$ and $0{\cdot}17$ volt.

(Goodman & Johnson, 1970). From such measurements made to date the value of V_{200} reduced to 0°K

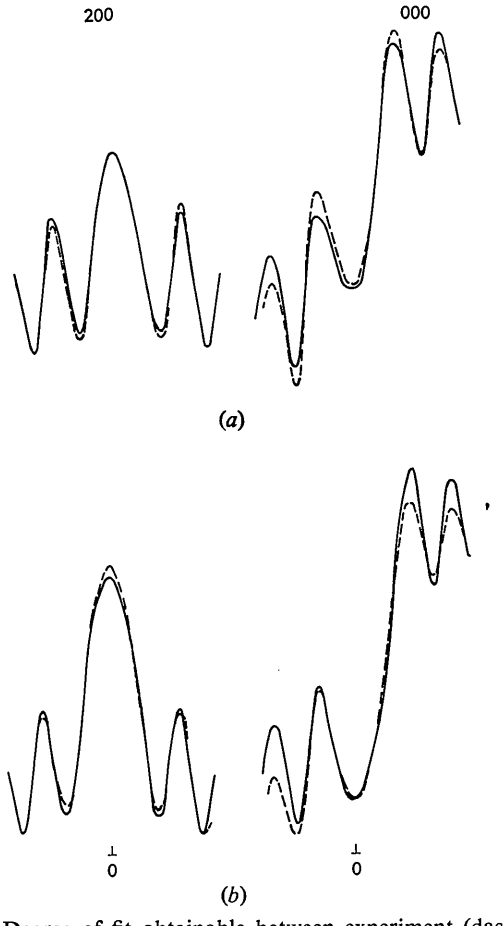

Fig. 2. Degree of fit obtainable between experiment (dashed curve) and calculation, for 000 and 200 beams. (E=79 kV, D=1115 Å). Data are from [026] region, (*a*) for $T=T_1$ and (*b*) for $T=T_2$. Values B=0·3, $V_h{}^t$=0·30 volt were used in (*a*), and B=0·9, $V_h{}^t$=0·36 volt in (*b*).

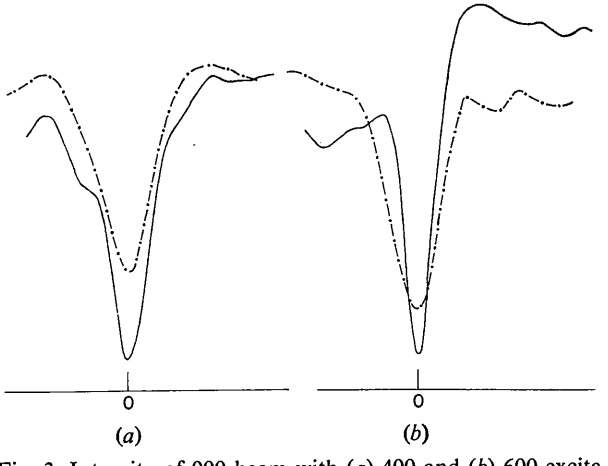

Fig. 3. Intensity of 000 beam with (*a*) 400 and (*b*) 600 excitation, at two temperatures, $T=T_1$ (full line) and $T=T_2$ (broken line).

i.e. $(V_{200})^0$ should lie in the range $(V_{200})^0=7{\cdot}05\pm0{\cdot}07$ volt. The effects on conclusions of changes in V_{200} within this range were then examined.

Experimental method

The specimen was heated by means of an addition to an early model of the tilting stage designed by Mills & Moodie (1968), which allowed a current to be passed through the specimen mesh, at the same time allowing an angular range sufficient to obtain the three principal axes [100] [110] and [111] from the one crystal.

The temperature was read in terms of heating current. The control was found to be reliable from the reproducibility of the results. A temperature range was determined for which conditions were stable (approximately 15 to 600°C). At lower temperatures contamination formed. During observations over a long period some crystals received radiation for an hour or more, and complete freedom from contamination was necessary in order to obtain reproducible results. At higher temperatures etching of the crystals under the beam occurred, although adjacent crystals remained unchanged at much higher temperatures. Rectangular pits and finally holes were produced in the crystals by etching. The etching could be controlled by lowering the temperature, to obtain thinned regions apparently perfect and parallel sided. However a useful range was found for which conditions were stable. During observation pictures were taken alternately at the two main temperatures used, *viz.* T_1 near room temperature and $T_2\simeq450$°C, to ensure that etching had not taken place. Accurate temperature measurement was not attempted. T_2 was chosen just below the point where incipient red emission was observed from the specimen support in the darkened room, which would appear to set an upper limit to the temperature, but reproducibility was obtained by reference to a stabilized current supply.

Analysis of systematic-interaction patterns

200 *patterns*

At first patterns with the 200 reflexion excited were examined. In particular the crystal later used in the zone-axis analysis was examined at the position of the crossing 082 line which fixed the orientation exactly, to obtain crystal thickness, and also B_1 and B_2 (for T_1 and T_2). The thickness was such that the condition was almost exactly at an extinction length ($D=2l_h$) for $T=T_1$. The effect of changing B factor on the 200 pattern is shown by means of the 4-beam systematic calculation in Fig. 1. At this condition the spacing of the subsidiary maxima is not much changed, but the central curve is affected. By comparison with the Patterns (see Fig. 8(*a*) and (*b*), Goodman, 1970) and assuming $B_1=0{\cdot}3$, B_2 can be obtained. A second measurement was made on a pattern with different condi-

tions, *viz.* $E=79$ kV, $D=1115$ Å, from the [026] region. The comparison of experiment and calculation is shown in Fig. 2.

In the case of the 082 pattern orientation was sufficiently well defined to allow 2-dimensional calculation with 109 beams to be made. This allowed an accurate thickness estimate, and *n*-beam interpretation for the extinction length. A value of $B_2=0{\cdot}7\pm0{\cdot}1$ was obtained from these measurements.

Finally an attempt was made to put the measurement of the systematic pattern on an absolute scale by recording the incident beam thus allowing determination of V_0', the zero-order absorption coefficient. Both before and after recording the crystal pattern the crystal pattern the crystal was moved just out of the beam and the incident cone recorded with a reduced exposure electronically controlled. In this way it was hoped to obtain transmission through carbon supporting film of the same thickness as that beneath the crystal. I_{000} was obtained from the pattern after first subtracting a smooth background obtained by continuing levels observed outside the *K–M* disc (*e.g.* see Fig. 10). Some inelastic scattering, *viz.* high-contrast characteristic loss scattering, is therefore probably present in the measurement, so giving a lower V_0' value than that for elastic scattering. The pattern measured was for the 082 line; with $E=79$kV, the values $V_0'=0{\cdot}6$, 0·7 volt, were obtained for $T=T_1$ and $T=T_2$, respectively using the 4-beam calculation with $V_h'=0{\cdot}25$ and 0·22, respectively (Goodman & Johnson, 1970).

400, 600 *patterns*

In the systematic-interaction case, as is well known, only the higher-order excitations are sensitive to the fall-off of V_h' with h, and have been used to test qualitatively the form of V_h' (Howie & Whelan, 1960; Goodman & Lehmpfuhl, 1967). In the present investigation the 000 beam asymmetry was examined for the 400 and 600 excitations at temperatures T_1 and T_2. It was found, for several positions on the Kossel map including those for which (*i.e.* the majority) an increase occurred with 200 excitation, that heating resulted in a marked *reduction* of the asymmetry. This result is shown for the [026] region in Fig. 3. If this were interpreted directly it would mean that the fall-off of temperature factor on V_h' greatly increased at T_2, and of course an increase is expected theoretically (Hall & Hirsch, 1965). However the apparent effect is increased by both accidental interactions, and probably thermal scattering. At low temperatures accidental interactions are influential; for the higher-order excitations the 000 asymmetry is seen to be a function of the sign of ζ_g for weak lines (Fig. 6(*d*) and (*e*), Goodman, 1970). At high temperatures the accidental influence is much reduced (*e.g.* Menzel-Kopp, 1962). Therefore this pattern is more suitable for systematic interpretation, provided the small contribution from thermal scattering of an opposite asymmetry can be allowed for. For the reasons given, evidence for the form of V_h' is sought, in preference, from the zone-axis pattern, particularly at the low temperature.

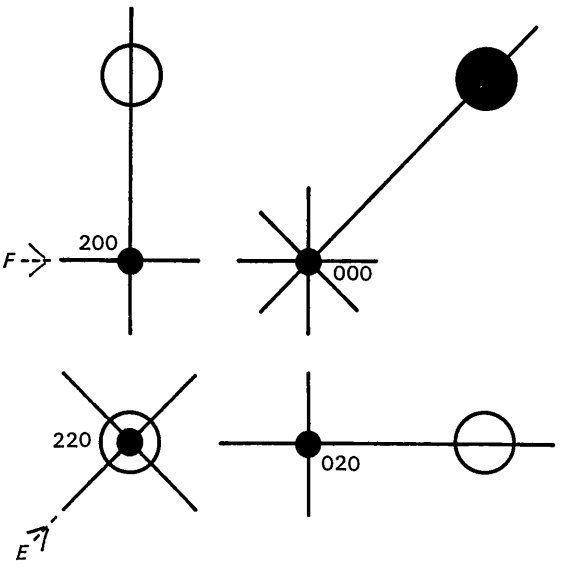

Fig. 5. Symmetry lines used for quantitative analysis and passing through the indexed reflexions are shown in relation to the zone-axis pattern.

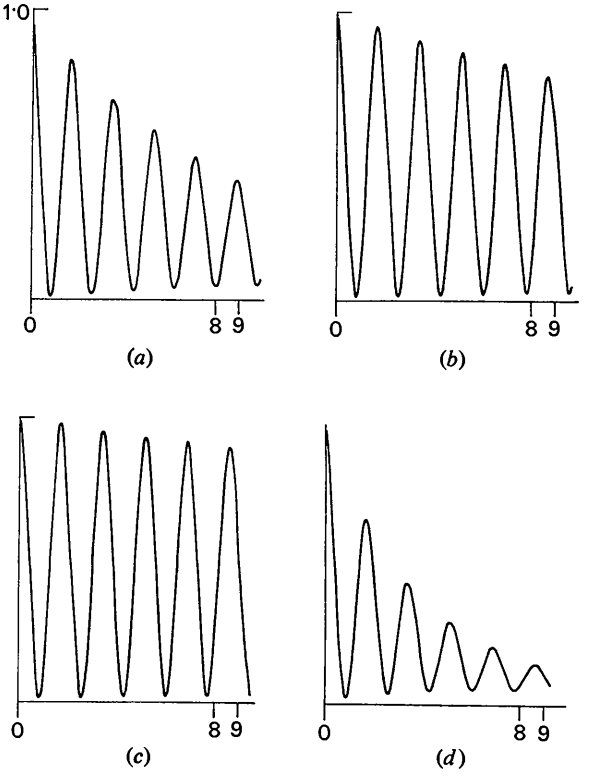

Fig. 6. Calculated thickness curves for 000 beam at the exact [001] zone axis. (*a*), (*b*) and (*c*) show the 69-, 109- and 129-beam calculations (see text) with $V_0'=V_h'=0$, and (*d*) the 129-beam calculation with $V_0'=0{\cdot}6$ volt, $V_h'=0{\cdot}14$ volt, $B'=0{\cdot}3$. Horizontal scale shows thickness in units of 100 Å.

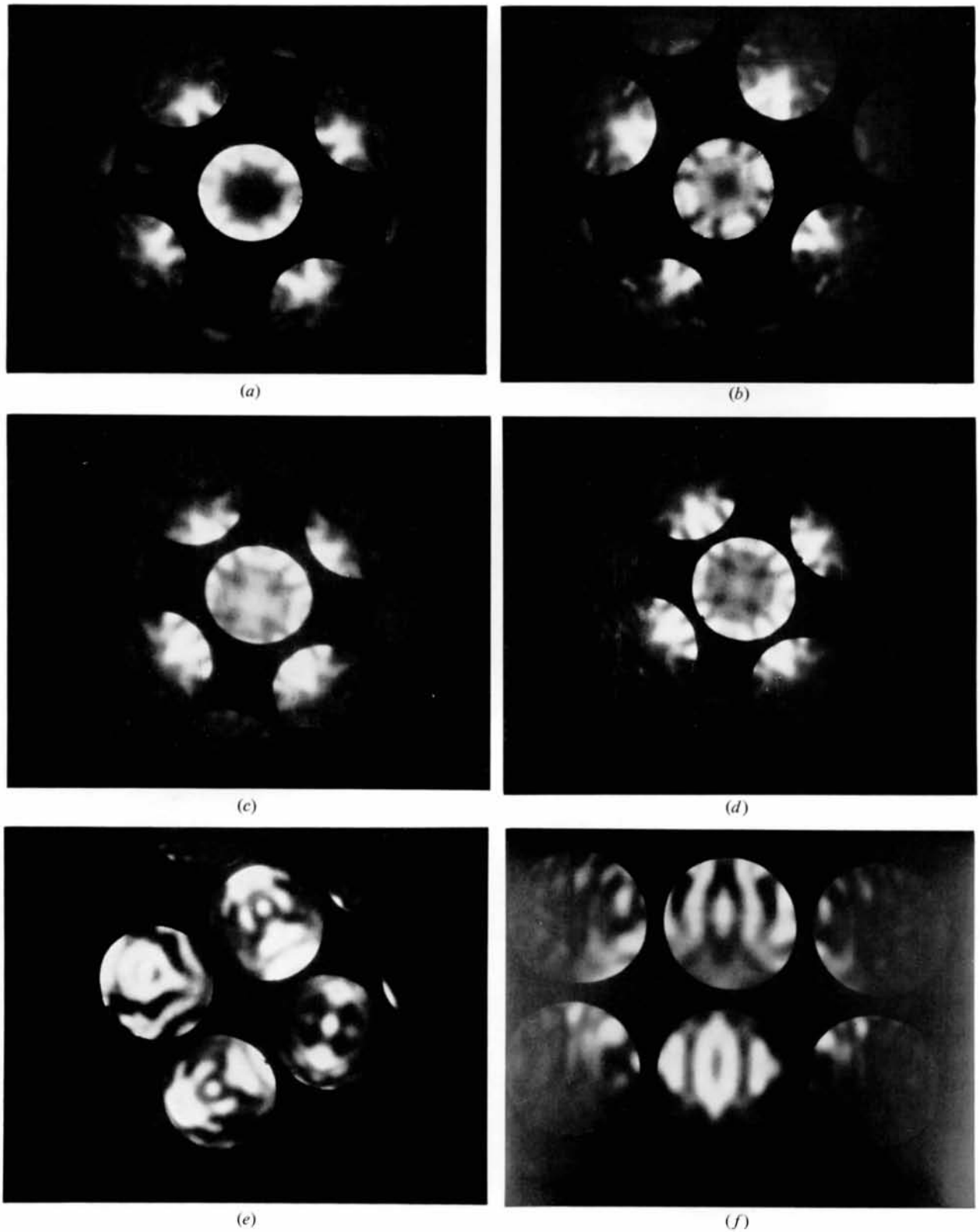

Fig. 4. Convergent-beam patterns near the [001] zone axis. (*a*) to (*d*) Incident beam symmetrical about [001]; (*a*), (*b*), $E=79$ kV and $T=T_1$, T_2, respectively; (*c*), (*d*), $E=105$ kV at the same temperatures. (*e*) Pattern for simultaneous excitation of 200, 020, 220, reflexions. (*f*) Symmetrical excitation of the 200 reflexion. (*e*) and (*f*) taken for $E=105$ kV. Crystal thickness was 890 Å.

[*To face p.* 142

Zone axis patterns

Pictures were taken at three different orientations near the [001] axis: the exact zone axis, symmetrical excitation of a single 200 reflexion, and satisfying 220, 200 and 020 reflexions simultaneously (Fig. 4). These patterns are relatively complicated when compared with the one-dimensional patterns which have been used in the past for quantitative work. It is informative at first to take the patterns at different wavelengths, and from different thickness. Details which are insensitive to wavelength will be also insensitive to structure factors (and also therefore to temperature factors), since the two parameters appear always in product in the n-beam solution (Cowley & Moodie, 1957). Near the [001] axis the interaction is so strong that the whole intensity distribution is affected by change of wavelength, but at the lesser poles [111] and [110] it is found by this experimental method that only the regions near $\zeta_h=0$ for a strong reflexion show any sensitivity to structure factor. Owing to the symmetries it is also seen that most of the useful information is obtained in one or two single line scans in certain directions across the patterns. Lines of symmetry were chosen for measurement, first because there are definite criteria to ensure that the orientation from which the data come is known with sufficient certainty, and secondly because the dynamic calculation is reduced by symmetry. The symmetry lines in the convergent beam pattern determined by the reciprocity law (Pogany & Turner, 1968) and the mirror planes of the structure are drawn in the different reflexions in Fig. 5. Quantitative analysis was attempted using as variables B, and V_h^i and B^i, assuming Fourier coefficients of absorption potential of the form $V_h^i \exp(-B^iS^2)$. It was not assumed that B^i and B were equivalent.

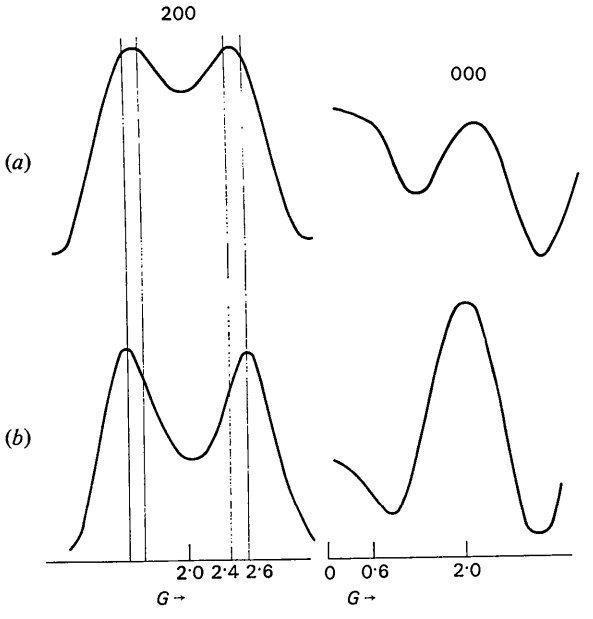

Fig. 7. Experimental curves with $E=105$ kV for line 'F' of Fig. 5, *i.e.* symmetrical excitation of the 200 reflexion. 200 and 000 intensities are shown (*a*) $T=T_1$ and (*b*) $T=T_2$. Vertical lines are included to show change peak separation for 200.

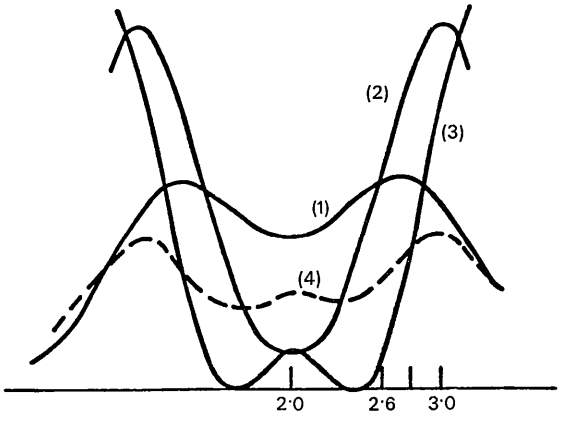

Fig. 8. Results of 69-beam calculation for the 200 beam in the symmetrical excitation for different values of B: (1) $B=0{\cdot}3$, (2) $B=0{\cdot}6$, (3) $B=0{\cdot}8$, with $V_h{}^i=0$, and (4) $B=0{\cdot}8$, $V_h{}^i=0{\cdot}6$ volt ($D=910$ Å, $E=105$ Å).

The accuracy of the calculation using the multi-slice method is limited by the number of beams considered and the slice thickness taken. In practice these two parameters are related. The latter value, Δz, is the distance over which the structure is projected, in the direction of propagation, to obtain the terms $Q_{(hk)}$ (Cowley & Moodie, 1957) used in the multi-slice convolution. It is not necessary for Δz to correspond to any real distance in the structure, but if beams are included of sufficient scattering angle, upper layer reflexions will be generated corresponding to the c spacing Δz. If the diameter of calculated diffraction pattern is to be increased, therefore, Δz must be decreased in order to prevent errors, until the true interatomic-layer value is reached. If at this stage the calculation is still insufficiently accurate potential slices must be taken which section the atomic layers. Sufficient accuracy is reached when a further change in this direction makes no significant change to the details being calculated. The accuracy required, in general, in determinations of absorption is much greater than that required in determining elastic scattering factors. In the present case exploratory calculations were first made with 69 beams and $\Delta z=7$ Å. With these values the calculation is still fairly rapid. After first conclusions had been reached, these were checked by second calculation with 109 beams and $\Delta z=4{\cdot}2$ Å. Calculation times were $(109/69)^2\times(7/4{\cdot}2)\simeq 4$ times longer, but were necessary to obtain the correct extinction lengths. Finally calculations were made for 129 beams and $\Delta z=2{\cdot}1$ Å, to obtain sufficient accuracy for absolute measurement of absorption. The normalization of the 129 beam calculation is 94% at 900 Å; in this calcula-

tion the slice thickness used is 2·1 Å, corresponding to single atom layer spacings. The only approximation remaining here is that identical atomic layers, containing mean atoms, (Mg+O)/2, have been used for convenience, so that those upper-layer reflexions with $h+k+l$ odd (weak reflexions) are omitted from calculation, which is a very good approximation for this projection. Thickness curves for [001], shown in Fig. 6, show the increasing accuracy and normalization with increased number of beams. The patterns with the two symmetries of '*F*' and '*E*' of Fig. 5 were analysed to show the separate influence of parameters *D* (thickness), *B*, V_h^i, B^i, by means of these calculations.

Pattern 'F': symmetrical excitation of 200

The crystal used for the patterns of Fig. 4, was first examined in the orientation defined by the 082 line as above. Using 109-beam calculation and $\Delta z = 2{\cdot}1$ Å, and the value $\{V_{200}\}^0 = 7{\cdot}0$ volt, the thickness for the extinction obtained ($D = 2l_h$), converted to the [001] direction, was 890 Å. This agreed closely with the value finally obtained from the [001] patterns. The pattern for line '*F*', of symmetrical excitation of 200, is taken from the two exposures of Fig. 4(*c*), (*d*) and (*f*) to obtain an angular range covering the zone-axis [001] and the $\zeta_{200} = 0$ peak. Experimental microphotometer curves for $T = T_1$, $T = T_2$, are shown in Fig. 7 for 000, 200.

The 200 curve, particularly the peak separation, is sensitive to *B*, but because of the complicated or non-periodic nature of the *n*-beam thickness curves, is not always very sensitive to thickness. Fig. 8 shows results from the preliminary 69-beam calculation for different *B*. Agreement with experimental peak separation for $T = T_1$ was obtained with $B = 0{\cdot}3$, $D \simeq 910$ Å for 69-beam calculation, but 890 Å for 109- or 129-beam calculation. Results for 200 at $T = T_2$ show increased peak separation and may be compared with calculation for different *B*. For $B = 0{\cdot}8$ a new maximum appears in the calculated curve (Fig. 8) even when V_h^i has a large value, which is not in the experimental curve and also the peak separation is too great. When the larger 109-beam calculation is made, and $\{V_{200}\}^0$ raised from 6·97 to 7·12 volts (at $T = T_1$) $B = 0{\cdot}8$ still gives no agreement, and a value $B_2 = 0{\cdot}6$ is obtained. For these *B* values little change is made to the calculated rocking curve shape by changes of *D* over a large range either side of the value 890 Å, showing an independence to any error in *D*, in contrast to the systematic interaction case. There appears to be agreement within $\simeq 0{\cdot}1$ between B_2 values determined near the zone axis and for the 'systematic' 082 case above. An effect still neglected is that the real term C_{oh}^r [Yoshioka & Kainuma's (1962) terminology] has increased significance with temperature, but this approach is consistent with this term being of second order compared with C_{oh}^i. Assuming that the present *n*-beam calculations are adequate, as indicated by Fig. 6, the systematic-interaction estimate is likely to be less satisfactory.* The value 0·6 is consistent for all the zone axis measurements and is in close agreement with

* *Note added*: In reference to the above, subsequent analysis showed that the systematic 4-beam calculation gave approximately 3% longer extinction length 11-beam systematic calculation at low temperature. The former is used only in preliminary analysis.

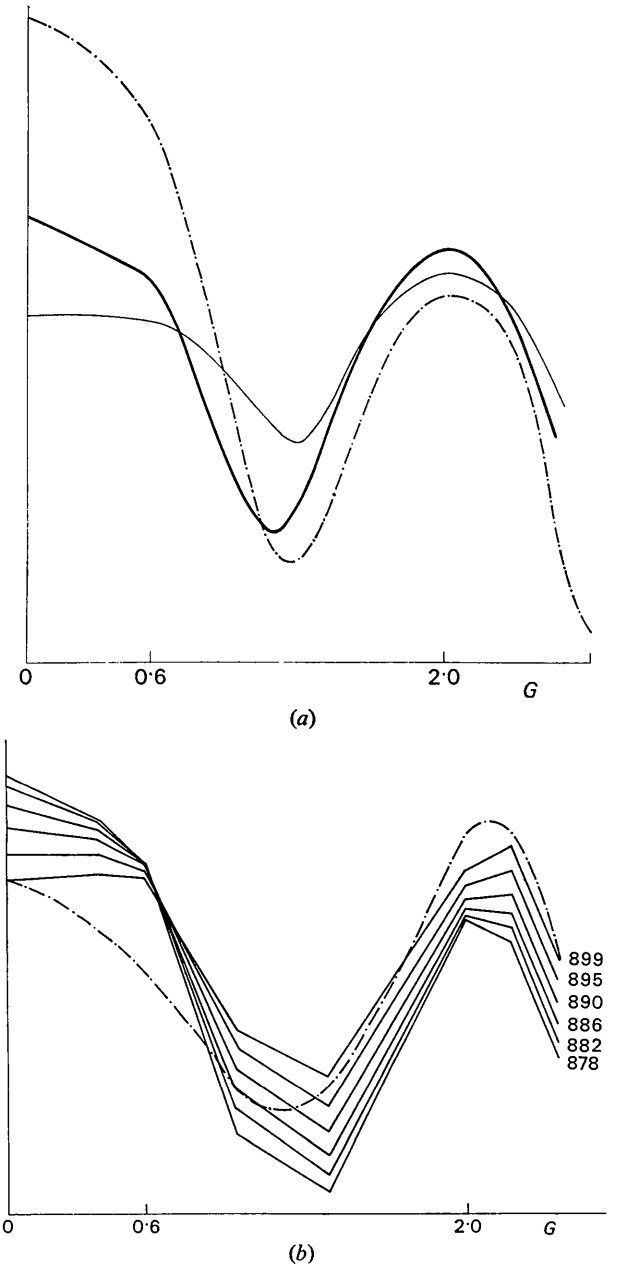

Fig. 9. (*a*) Results of 109-beam calculation for 000 beam with different absorption models having $V_h^i = 0{\cdot}14$ volt and $V_0^i = 0{\cdot}6$ volt: $B^i = 0{\cdot}3$ (heavy full line); $B^i = 0{\cdot}8$ (chain line), both with $B = 0{\cdot}3$. Light full line shows results for $B = 0{\cdot}2$, and same absorption parameters as heavy full line. (*b*) Calculation with 129 beams for different thicknesses shown next to curves in ångströms, in single unit cell steps, ($V_h^i = 0{\cdot}14$ volt, $V_0^i = 0{\cdot}6$ volt, $B^i = 0{\cdot}3$). Chain line shows result of chaging only V_h^i to 0·18 volt.

X-ray values. It is shown that conclusions given here concerning the high temperature absorption function are not dependent upon this value.

The 000 curve contains more information than the 200 curve, and is sensitive to D, B, V_h^I and B^I. The patterns were measured on an absolute scale (for background subtraction see Fig. 10), in the way described above so that V_0^I could be determined. Patterns were taken for 105 and 79 kV; only the former were analysed in detail. Discussing first the absorption function

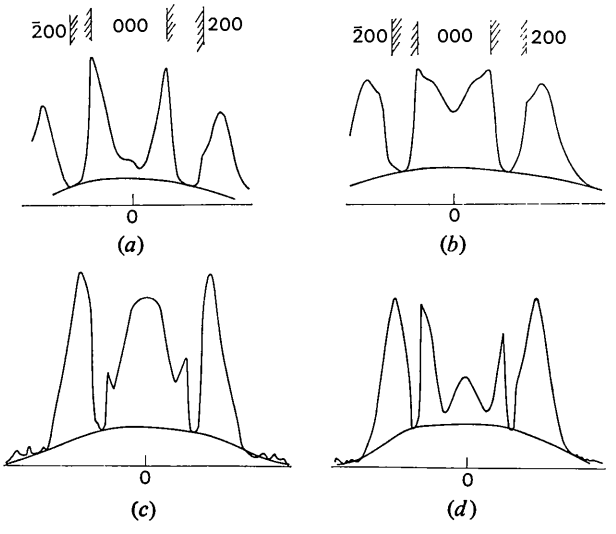

Fig. 10. (*a*) to (*d*). Experimental curves from the symmetrical setting for 200, 000, 200, beams taken along line '*F*', from Fig. 4(*a*) to (*d*) respectively. Continuous background, determined from intensity level between reflexions, is shown drawn in.

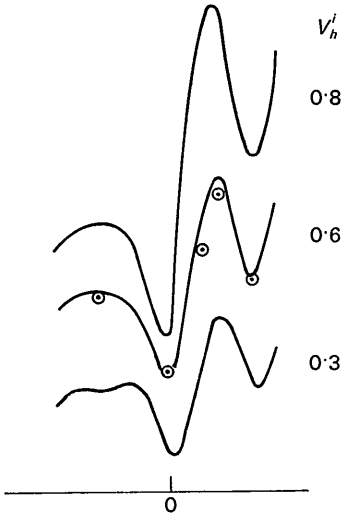

Fig. 11. 69-beam calculations for 000 curve for the line '*E*' of Fig. 5 passing through ζ_{200}, ζ_{020}, $\zeta_{220}=0$, for different values of $V_h{}^I$ viz: 0·3, 0·6, 0·8 volts, and $B=0{\cdot}5$. Similar curves, with slightly different $V_h{}^I$ values, are obtained with B values between 0·5 and 0·8. Encircled points show comparison with 109-beam calculation, not on an absolute basis.

it is seen that V_h^I and B^I affect the intensity in different ways. At [001] I_{000} is closely cosinusoidal with thickness as in the 2-beam solution, but now we have the two absorption parameters: V_h^I affects both maxima and minima of the thickness curve and B^I affects mainly the maxima. In the rocking curve when this includes both [001] and $\zeta_{200}=0$, V_h^I and B^I may be separated from single-thickness data. This is shown in Fig. 9. Sensitive points on the curve are at $G=0{\cdot}0$, 0·6, 2·0, on the horizontal scale ($G=0{\cdot}0$, 2·0, correspond to [001] and $\zeta_{200}=0$, respectively), particular features being a broad peak at $G=0{\cdot}0$ and an inflexion at $G=0{\cdot}6$. For $V_0^I=0{\cdot}6$ volt, $V_h^I=0{\cdot}14$ volt, $B^I=0{\cdot}3$, the experimental curve is reproduced (109-beam calculation). Increasing B^I to 0·8 and leaving V_h^I at 0·14 volt increases $I_{(0{\cdot}0)}$, slightly lowers $I_{(2{\cdot}0)}$ and removes the inflexion at $G=0{\cdot}6$ [Fig. 9(*a*)]. Increasing now V_h^I to 0·18 volt restores agreement near $G=2{\cdot}0$ but not near 0·0 and 0·6. When V_h^I is decreased to 0·18 and B^I left at 0·3, $I_{(0{\cdot}0)}$ is reduced, the inflexion at $G=0{\cdot}6$ removed and $I_{(2{\cdot}0)}$ increased [see Fig. 9(*b*)]. Therefore $V_h^I=0{\cdot}14\pm0{\cdot}02$ volt, and $B^I\simeq B$.

Agreement was possible within the range $\{V_{200}\}^0=7{\cdot}05\pm0{\cdot}07$ volt. Calculations were run for $B=0{\cdot}3$, 0·25, 0·2, with fixed V_{200}. Agreement was best for 0·3 and worst for 0·2 [see Fig. 9(*a*)].

The more accurate 129-beam calculation was run. Results for $B=0{\cdot}3$, $V_h^I=0{\cdot}14$, $B^I=0{\cdot}3$, as in Fig. 9(*a*), are shown in Fig. 9(*b*). Firstly, the sensitivity to thickness is shown; D can be refined to 890 ± 4 Å. Secondly, the relative curve shape has changed very slightly, moving the absorption estimates in the direction $V_h^I\simeq0{\cdot}15$ volt (to within an accuracy of 0·01 volt for V_h^I however the reproducibility of temperature is scarcely sufficient). Also the value $V_0^I=0{\cdot}6$ volt gives 12% of incident energy at $\zeta_{200}=0$, in good agreement with the measured value (Table 1).

Table 1. *Measured values for* I_{000} *(intensity of central beam) obtained from Fig.* 10, *expressed as a percentage of incident energy, for the two temperatures*

	T_1	T_2
105 kV; $\zeta_{2000}=0$	12½%	23%
79 kV [001]	1–2	4

Additional observation at 79 kV

When E is changed to 79 kV in the calculation with $B=0{\cdot}3$, $D=890$ Å, the observed zone axis rocking curve, with a small central maximum [$T=T_1$; Fig. 10(*c*)], is reproduced. This gives a check on these parameters. Measurements of intensity minimum for I_{000} above background [Fig. 10(*c*)] gives $\simeq1\%$ of the incident energy (Table 1). This measurement of a small quantity is made relatively accurate by using an electronically reduced exposure of the incident beam for comparison. Thus it is significantly less than the value of 3½% transmission obtained by a 129-beam calcu-

lation at the values $V_0=0{\cdot}6$ volt, $V_h^i=0{\cdot}14$ volt, $B^i=0{\cdot}3$; the measured value is very little greater than the transmission calculated for $V_h^i=0$. However in this case the method of subtracting background may be at fault. Near the 000 beam at the zone axis, a minimum in the diffuse intensity may occur dynamically due to the anti-phase nature of thermal scattering (*cf.* Gjønnes & Moodie, 1965). By electronic → thermal scattering the total diffuse scattering may also have a minimum at [001]. This would account for the low minimum measured by assuming a smooth background.

Summary

The value $V_h^i=0{\cdot}14$ volt, is a little lower than the value measured for 105 kV near the zone axis for the systematic case (Goodman & Johnson, 1970), but this is understandable since the weak-beam effects are included in the complete calculation. It does not appear increased near the zone-axis, and along the symmetry line for single excitation of the 200 reflexion. This seems to be consistent with the fact that no other Kossel lines are crossed, and with the rule deduced from other observations (and consistent with a very localized concentration of thermal scattering around Bragg points) that V_h^i is increased dynamically only close to Kossel line intersections.

The observation that $B^i=B$ is consistent with absorption from thermal scattering (*i.e.* a rigid ion approximation), and may also be close to the situation for core excitation losses, since the inner-electron volume is relatively small.

The value for V_0 of 0·6 volt at 105 kV may be slightly less than the value appropriate for purely elastic scattering, since the present simple background subtraction may leave some low-angle inelastic scattering in the measurement.

The B value of 0·3 near room temperature is consistent with X-ray values (Dawson, 1969). Also, using the approximate estimate of 450°C the value of 0·6 for $T=T_2$ is close to agreement with X-ray measurements (Baldwin & Thompson, 1964). For the purpose of obtaining a plot of characteristic temperature however it is seen that the simpler [111] projection for which all V_h are known would be more suitable, and that better temperature calibration would be required.

Pattern 'E': simultaneous excitation of 200, 020, 220

This pattern is shown in Fig. 4(*e*). Preliminary experimental investigation, changing λ, and D, showed that the actual positions of the maxima and minima in the Kossel–Möllenstedt pattern was relatively independent of λ and mainly thickness dependent (Fig. 11). However the relative shape of the 000 curve measured along the symmetry line 'E' was particularly sensitive to temperature. The experimental results for T_1 and T_2 along line E, showing a large increase of asymmetry between temperatures are seen in Fig. 12. The pattern for $B=0{\cdot}3$ is complicated and the asymmetry is not a simple function of V_h^i in the calculation. However approximate agreement with experiment is obtained using the values for V_h^i, B, *etc.* found above, from the pattern 'F', for the temperature T_1 [Fig. 12(*a*)]. For $B>0{\cdot}45$ (and for $E=105$ kV, $D=890$ Å), the 000 asymmetry is mainly a function of V_h^i, only secondarily a function of B, and relatively insensitive to B^i. Therefore the point given by Yoshioka & Kainuma (1962), of dynamical increase of V_h^i near an n-beam intersection could be tested. This is done by considering the high-temperature patterns for the two orientations, and interpreting with the function $V_h^i \exp(-BS^2)$ which was tested for $T=T_1$, in the 109-beam calculation. To obtain the observed asymmetry a high value, $V_h^i \simeq 0{\cdot}75$ volt, is required for pattern 'E' if $B=0{\cdot}6$, compared with $V_h^i \simeq 0{\cdot}25$ volt for the previous, single excitation, pattern. If $B>0{\cdot}6$ because of an error in the determination *e.g.* $B=0{\cdot}8$, V_h^i is lowered to $\simeq 0{\cdot}6$ volt but also V_h^i for the single excitation pattern is lowered. It is emphasized that these results are obtained from the relative intensities and not absolute intensities as in the previous section, so that V_h^i was not measured.

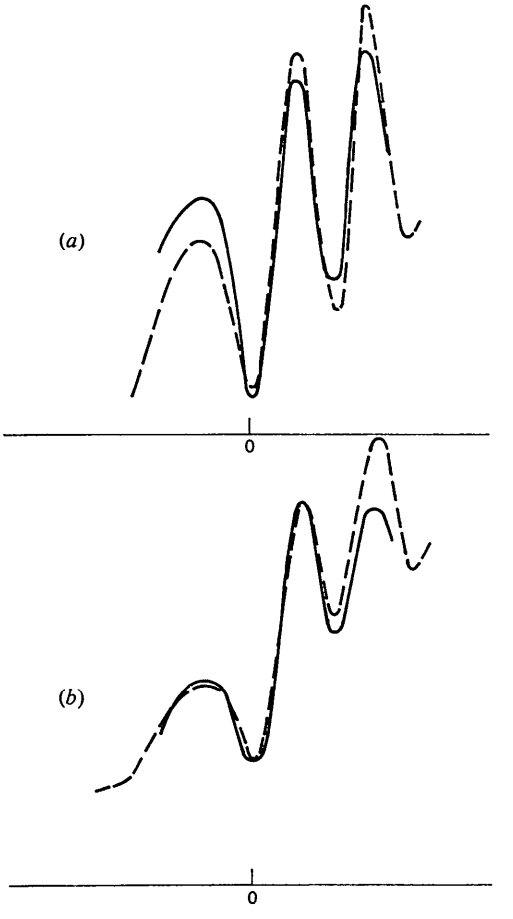

Fig. 12. Experimental (dashed line) curves for 000 beam taken from the line 'E' with simultaneous 3-reflexion excitation. (*a*) for $T=T_1$ is shown together with calculated 109-beam curve with $V_h{}^i=0{\cdot}14$ volt, $B^i=B=0{\cdot}3$. (*b*) for $T=T^2$ together with calculated curve for $V_h{}^i=0{\cdot}8$ volt, $B^i=B=0{\cdot}5$.

Also the local diffuse scattering was not subtracted. It seems difficult to believe that the observed asymmetry is due to thermal scattering, and rather the reverse asymmetry might be expected from this source; therefore this curve was interpreted phenomenologically. Experimentally this effect was checked by cycling between the two temperatures, and patterns taken over a period of a few days were reproducible except for small differences attributable to the extreme sensitivity of the pattern to temperature. However the same large change with temperature was not observed in some crystals of other thicknesses, showing that the dynamic problem is quite complicated. Finally the value of $\{V_{200}\}^0$ was changed in the (109-beam) calculation, from 6·97 to 7·12 volt (2%), covering the maximum probable range. This changed mainly the intensity of the zone axis. Now V_h' for the single excitation was raised to 0·35 volt (see Fig. 13) and 0·75 volt for the 3-reflexion pattern. It was concluded that the phenomenological V_h' was between two and three times greater near the 3-reflexion excitation at high temperature.

Summary

Results for the high temperature, $T \simeq 450\,^{\circ}C$, indicate that the V_h' value is two to three times greater near the 3-line (4-beam) intersection 200, 020, 220, compared with the value for single 200 excitation. The explanation seems to be that, considering the thermal scattering to be concentrated around the Bragg points, when ζ_{200}, ζ_{020}, ζ_{220} change sign simultaneously a large amount of thermal scattering moves from outside to inside the Ewald sphere. There is some current discussion as to whether such effects are all taken into account by the full dynamical calculation and fixed coefficients V_h', and this would appear to be true for an Einstein distribution. The degree to which V_h' will be increased would appear to depend upon the degree of localization of the actual thermal scattering distribution. Furthermore, observations made on simpler patterns, such as the high anomalous transmission observed near the 082 line (Goodman, 1970), are difficult to explain without postulating some increase in V_h' close to the 3-line intersections. The temperature at which such effects are observable appears to depend upon whether high- or low-index reflexions are involved.

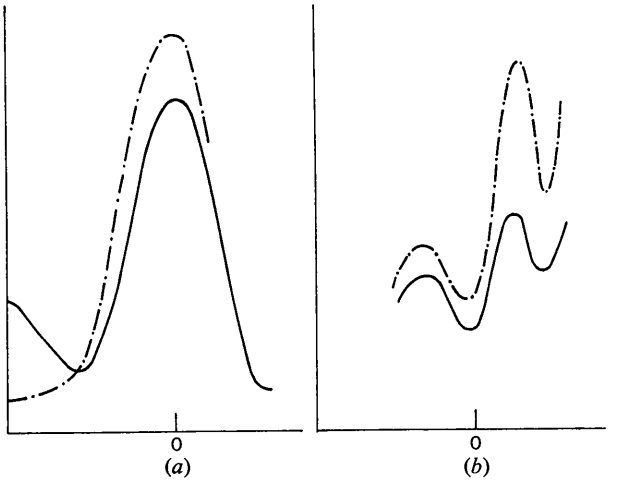

Fig. 13. (*a*) Calculations for comparison with high-temperature patterns (T_2) assuming $(V_{200})^0 = 7{\cdot}12$ volt and $B = 0{\cdot}6$, for single 200 excitation. (*b*) for 3-reflexion excitation.
Full line: $V_h' = 0{\cdot}35$ volt; chain line: $V_h' = 0{\cdot}75$ volt. (*a*) and (*b*) may be compared in shape with the experimental distributions in Fig. 12(*b*) and Fig. 7(*b*).

In conclusion, the author would like to express his indebtedness to others. In particular to Professor J. M. Cowley for discussions on this work over a long period, to Mr A. F. Moodie and Dr A. W. S. Johnson for assistance during the project, and to Dr P. A. Doyle for his critical reading and correcting of the first draft.

References

BALDWIN, T. O. & TOMPSON, C. W. (1964). *J. Chem. Phys.* **41**, 1420.
COWLEY, J. M. & MOODIE, A. F. (1957). *Acta Cryst.* **10**, 609.
DAWSON, B. (1969). *Acta Cryst.* A**25**, 12.
GJØNNES, J. & MOODIE, A. F. (1965). *Acta Cryst.* **19**, 65.
GOODMAN, P. (1970).
GOODMAN, P. & JOHNSON, A. W. S. (1970). To be published.
GOODMAN, P. & LEHMPFUHL, G. (1967). *Acta Cryst.* **22**, 14.
HALL, C. R. & HIRSCH, P. B. (1965). *Proc. Roy Soc.* A**286**, 158.
HOWIE, H. & WHELAN, M. J. (1960). *Proc. European Regional Conf. Electron Microscopy, Delft*, p. 181.
MENZEL-KOPP, C. (1962). *J. Phys. Soc. Japan*, **17**, B11.
MILLS, J. C. & MOODIE, A. F. (1968). *Rev. Sci Instrum.* **39**, 962.
POGANY, A. P. & TURNER, P. S. (1968). *Acta Cryst.* A**24**, 103.
TOGAWA, S. (1964). *J. Phys. Soc. Japan*, **20**, 742.
YOSHIOKA, H. & KAINUMA, Y. (1962). *J. Phys. Soc. Japan*, **17**, B11, 134.